Vítor Monteiro, Tiago Sousa, João L. Afonso

“A Novel Topology of Modular Multilevel Bidirectional Non-Isolated dc-dc Converter,”

YEF-ECE International Young Engineers Forum on Electrical and Computer Engineering, Almada Portugal (virtual conference), July 2020.

Vítor Monteiro, Tiago Sousa, João L. Afonso, "A Novel Topology of Modular Multilevel Bidirectional Non-Isolated dc-dc Converter," YEF-ECE International Young Engineers Forum on Electrical and Computer Engineering, Almada Portugal (virtual conference), July 2020.

A Novel Topology of Modular Multilevel Bidirectional Non-Isolated dc-dc Converter

Vitor Monteiro
Centro ALGORITMI
University of Minho
Guimaraes, Portugal
vmonteiro@dei.uminho.pt

Tiago J. C. Sousa
Centro ALGORITMI
University of Minho
Guimaraes, Portugal
tsousa@dei.uminho.pt

Joao L. Afonso
Centro ALGORITMI
University of Minho
Guimaraes, Portugal
jla@dei.uminho.pt

***Abstract*—The paradigm of smart grids has been continuously addressing new challenges in terms of power electronics converters, for instance, to deal with technologies like renewables, electric mobility, energy storage, and hybrid power grids. Allied with this context, a novel topology of modular multilevel bidirectional (MMB) non-isolated dc-dc converter is proposed in this paper. Taking into consideration the nature of the proposed MMB dc-dc converter, it is appropriated to operate as back-end converter linked to front-end ac-dc converters based on cascade structures, i.e., with more than one dc-link. As distinctive features, the proposed MMB dc-dc converter can operate with five-voltage levels, allowing to reduce the voltage stress in each semiconductor, and it is controlled based on the interleaved principle of operation, although it is not an interleaved converter. A dedicated pulse-width modulation, as well as voltage and current control strategies, are proposed and clearly explained along the paper. The claimed distinctive features of the proposed MMB dc-dc converter are supported by analytic description and by computer simulation validation, considering steady-state and transient-state operations in relevant conditions of the dc interfaces.**

***Keywords*—Dc-dc Converter, Modular Converter, Multilevel Converter, Bidirectional Converter, Non-Isolated Converter.**

I. INTRODUCTION

Nowadays, the production, transportation, and distribution sectors are engaged with emerging technologies toward to lead with environmental concerns, where special focus is given to new paradigms of smart grids, including smart homes, electric mobility and renewables [1][2][3]. Consequently, it is foreseen that, even further, these technologies contribute to involve smart cities within smart grids [4]. Analyzing in more detail the required power interfaces, it is well identified the power electronics as a central technology. In this perspective, a study regarding the solicitation of innovative power electronics technologies in the perspective of smart grids is considered in [6], an overview concerning power quality issues and control technologies from the smart grid point of view is presented in [7], and a role of power electronics in future smart grids is analyzed in [5]. Nevertheless, the application of power electronics is very vast and embraces distinct areas as: solid-state transformers at distribution level [8]; integrated topologies for renewables [9]; hybrid ac-dc power grids [10]; protection technologies for dc microgrids [11]; electric vehicle (EV) fast chargers [12]; EV operation modes for supporting the power grid [13]; high-voltage dc grids [16]; and new power converters with improved control stratagems [14]. Scrutinizing the constitution of these areas regarding power stages, the use of dc-dc converters is a common feature, permitting to establish different levels of voltage/current controllability, both in buck or boost power stages. A comprehensive overview regarding bidirectional dc-dc power converters, including topologies and control patterns, is presented in [15]. According to the application requirements, there are numerous topologies of dc-dc power converters, each one presenting advantages and disadvantages, but none of them covers all the characteristics of the one proposed in this paper, i.e., a non-isolated modular, multilevel and bidirectional (MMB) dc-dc converter.

As differentiating aspects of the proposed MMB dc-dc converter, it can be highlighted: (a) Operation with two dc interfaces, however, one of the interfaces has two dc-links, each one with split capacitors; (b) Bidirectional operation, controlled in buck-mode (with voltage or current feedback) or controlled in boost-mode (also with voltage or current feedback); (c) Operation with multilevel voltage, allowing to produce up to five different voltage levels, depending on the voltage levels assumed by each dc interface (independently of the operation in buck-mode or boost-mode); (d) Operation in interleaved mode, regardless of the operation in buck-mode or boost-mode, allowing to control the variables (voltage or current) to present a ripple whose frequency corresponds to four times the switching frequency; (e) Combination of the previous cases, e.g., the converter can operate in buck-mode with current control, as well as with multilevel characteristics (which can change according to the voltage levels assumed by each dc interface) and with interleaved characteristics.

The proposed MMB dc-dc converter can be used for several purposes of power electronics in smart grids, as example: (a) Interface between energy storage systems in EVs; (b) Interface between active rectifiers (ac-dc) based on cascade structures and single dc interface; (c) Interface of renewable energy sources and grid-tied inverters (dc-ac) based on cascade structures. The proposed dc-dc converter can be used for a wide range of applications, where an illustrative example is presented in Fig. 1. As shown in Fig. 1(a), when a cascade ac-dc converter is considered, the dc-side has two individual dc-links, which is limitative for several applications (even using two individual dc-dc converters). On the other hand, by using the proposed MMB dc-dc converter, it is possible to

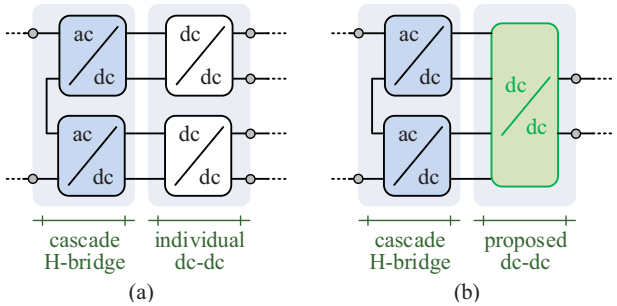

Fig. 1. (a) Cascade ac-dc converter with two individual dc-links and two dc-dc converters; (b) Illustrative example of application for the proposed MMB dc-dc converter.

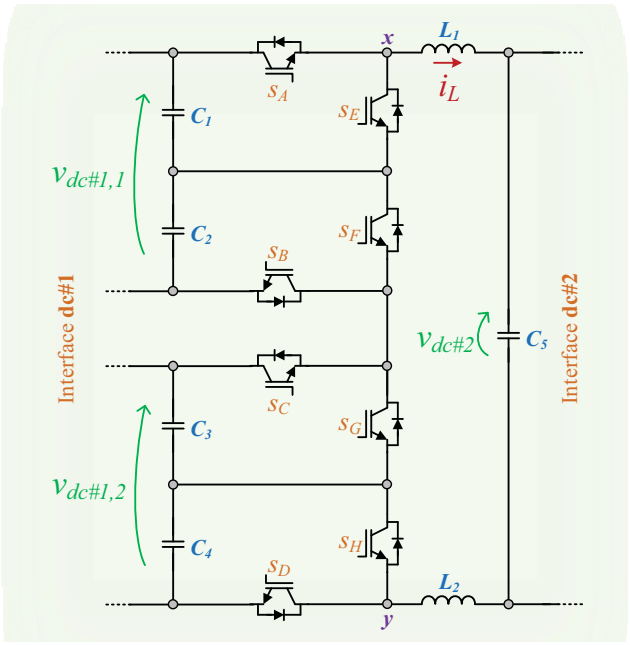

Fig. 2. Topology of the proposed non-isolated, modular, multilevel and bidirectional (MMB) dc-dc converter.

obtain a single dc-link on the dc-side, as shown in Fig. 1(b). Fig. 2 shows the proposed MMB dc-dc converter, which is constituted by eight fully-controlled semiconductors (IGBTs in this case), all of them individually controlled, but in groups of four, i.e., the IGBTs s_A to s_D are controlled during the buck-mode and the IGBTs s_E to s_H are controlled during the boost-mode. An L filter (L_1 and L_2) is considered in the interface dc#2 due to its simplicity of analysis in terms of control and modulation. The rest of the paper is arranged as follows. Section II introduces the principle of operation. Section III presents the current and voltage control equations based on a digital implementation, as well as the details of the modulation. Section IV presents the validation of the distinct operation modes in buck-mode and boost-mode, considering steady-state and transient-state. Section V ends the paper with the main conclusions.

II. Proposed MMB dc-dc Converter: Principle of Operation

As shown in Fig. 2, the proposed MMB dc-dc converter is constituted by two groups of IGBTs, which are used, respectively, during the buck-mode (s_A, s_B, s_C, s_D) and during the boost-mode (s_E, s_F, s_G, s_H), and, due to the voltage symmetry in the IGBTs, it is classified as symmetrical. As shown, the proposed MMB dc-dc converter is constituted by two dc interfaces, namely dc#1 or dc#2, although the interface dc#1 has two distinct parts (corresponding to the voltages $v_{dc\#1,1}$ and $v_{dc\#1,2}$). When the proposed MMB dc-dc converter operates in buck-mode, it means that the power follows from the interface dc#1 to the interface dc#2, while when it operates in boost-mode, it means that the power follows from the interface dc#2 to the interface dc#1.

During the operation in buck-mode, the average value of the current in the IGBTs s_A to s_D ($\overline{I}_s$) is calculated based on a function of the duty-cycle (D) and the current on the L filter ($\overline{I}_{L\{1,2\}}$), according to:

$$\overline{I}_{s\{A,B,C,D\}} = D\,\overline{I}_{L\{1,2\}}\,, \tag{1}$$

while for the IGBTs s_E to s_H is calculated according to:

$$\overline{I}_{s\{E,F,G,H\}} = (1-D)\overline{I}_{L\{1,2\}}\,. \tag{2}$$

On the other hand, during the operation in boost-mode, the average value of the current in the IGBTs s_A to s_D is calculated according to:

$$\overline{I}_{s\{A,B,C,D\}} = (1-D)\,\overline{I}_{L\{1,2\}}\,, \tag{3}$$

while for the IGBTs s_E to s_H is calculated according to:

$$\overline{I}_{s\{E,F,G,H\}} = D\,\overline{I}_{L\{1,2\}}\,. \tag{4}$$

Concerning the average value of the voltage in each IGBT ($\overline{v}_s$), during the operation in buck-mode, for the IGBTs s_A to s_D it is obtained as follows:

$$\overline{v}_{s\{A,B,C,D\}} = \frac{1}{2}\overline{v_{dc}}_{\{\#1,\#2\}} - \overline{v}_{s\{E,F,G,H\}}\,. \tag{5}$$

while for the IGBTs s_E to s_H is calculated according to:

$$\overline{v}_{s\{E,F,G,H\}} = \frac{1}{2}\,\overline{v_{dc}}_{\{\#1,\#2\}}\,, \tag{6}$$

On the other hand, during the operation in boost-mode, the average value of the voltage in the IGBTs s_A to s_D is calculated according to:

$$\overline{v}_{s\{A,B,C,D\}} = \frac{1}{2}\,\overline{v_{dc}}_{\{\#1,\#2\}}\,, \tag{7}$$

while for the IGBTs s_E to s_H is calculated according to:

$$\overline{v}_{s\{E,F,G,H\}} = \frac{1}{2}\overline{v_{dc}}_{\{\#1,\#2\}} - \overline{v}_{s\{A,B,C,D\}}\,. \tag{8}$$

By analyzing equations (1) to (8), it is recognized that the operations with values of duty-cycle near 50% are the most beneficial in order to balance the currents and voltages in all the IGBTs. The same situation occurs when both dc#1 and dc#2 interfaces are operating with similar values of voltage. Consequently, it is possible to define objectives for optimizing the losses through the IGBTs.

III. Proposed MMB dc-dc Converter: Control and Modulation

Based on the analysis of Fig. 2, it can be seen that both dc#1 and dc#2 interfaces are controlled separately, considering voltage or current strategies.

A. Buck-Mode Operation

1) Current Control and Modulation

Considering the interface dc#1 as the input-side (source) and the interface dc#2 as the output-side (load), the relation of voltages on the output-side is established as:

$$v_{L1}(t) + v_{L2}(t) + v_{dc\#2}(t) - v_{xy}(t) = 0\,, \tag{9}$$

where v_{xy} denotes the voltage level of the dc-dc converter (voltage measured between the points *x* and *y*), $v_{dc\#2}$ denotes the voltage of the interface dc#2, and $v_{L\{1,2\}}$ denotes the voltage in the inductors L_1 and L_2. By substituting the voltage in the inductors, yields:

$$L_1 \frac{di_{L1}(t)}{dt} + L_2 \frac{di_{L2}(t)}{dt} + v_{dc\#2}(t) - v_{xy}(t) = 0 \tag{10}$$

where, by applying the forward Euler method and knowing that the current in both inductors is the same, the digital implementation results in:

$$L_{\{1,2\}} \frac{\left(i_{L\{1,2\}}[k+1] - i_{L\{1,2\}}[k]\right)}{T_s} + v_{dc\#2}[k] - v_{xy}[k] = 0\,. \tag{11}$$

The current in the instant [k+1] corresponds to the current that must be reached in the period [k, k+1]. So, the reference current must be considered instead of $i_{L\{1,2\}}[k+1]$. With the objective of controlling the current in the period [k, k+1], the voltage $v_{xy}[k]$ is the reference that the MMB dc-dc converter must synthesize during such period. Taking into account that the proposed MMB dc-dc converter is controlled as an interleaved topology, the same reference voltage is compared with four carriers (shifted by 90 degrees between each other and with the same frequency and amplitude). In this case (buck-mode operation), only the IGBTs s_A to s_D are controlled, while the IGBTs s_E to s_H are turned-off.

2) Voltage Control and Modulation

Considering the voltage control in buck-mode, the following relation can be established:

$$v_{dc\#2} = D\left(\frac{v_{dc\#1,1}}{2} + \frac{v_{dc\#1,2}}{2}\right). \tag{12}$$

B. Boost-Mode Operation

1) Current Control and Modulation

Considering the interface dc#2 as the input-side (source) and the interface dc#1 as the output-side (load), the relation of voltages on the output-side is established as:

$$v_{L1}(t) + v_{L2}(t) - v_{dc\#2}(t) - v_{xy}(t) = 0\,, \tag{13}$$

where v_{xy} denotes the voltage level of the dc-dc converter (voltage measured between the points *x* and *y*), $v_{dc\#2}$ denotes the voltage of the interface dc#2, and $v_{L\{1,2\}}$ denotes the voltage in the inductors L_1 and L_2. By substituting the voltage in the inductors and applying the forward Euler method, the digital implementation results in:

$$L_{\{1,2\}} \frac{\left(i_{L\{1,2\}}[k+1] - i_{L\{1,2\}}[k]\right)}{T_s} - v_{dc\#2}[k] - v_{xy}[k] = 0\,. \tag{14}$$

The analysis performed during the operation in buck-mode is also applied during the boost-mode regarding the reference voltage that is compared with the carriers, as well as the characteristics of the four carriers (shifted by 90 degrees between each other and with the same frequency and amplitude). However, in this case, as the MMB dc-dc converter is operating in boost-mode, only the IGBTs s_A to s_D are controlled, while the IGBTs s_E to s_H are turned-off.

2) Voltage Control and Modulation

Considering the voltage control in boost-mode, the following relation can be established:

$$\left(\frac{v_{dc\#1,1}}{2} + \frac{v_{dc\#1,2}}{2}\right) = \frac{v_{dc\#2}}{(1-D)}\,. \tag{15}$$

IV. Proposed MMB dc-dc Converter: Validation of Operation Modes

The main results obtained for validating the MMB dc-dc converter are presented in this section. The validation was carried out according to a simulation model developed in PSIM v9.1. With the objective of obtaining realistic conditions of operation, distinct voltage levels were considered in both dc interfaces, therefore, it was possible to validate the multilevel feature of the proposed dc-dc converter. The switching frequency was fixed at 20 kHz and the control algorithm was executed with a sampling frequency of 40 kHz. In terms of passive elements, it was considered: $L_{\{1,2\}} = 500$ µH and $C_{\{1,2,3,4,5\}} = 100$ µF.

Fig. 3 shows the principle of operation of the pulse-width modulation (PWM) proposed for the MMB dc-dc converter, assuming as an exemplificative case a duty-cycle reference of 75% during the operation in buck-mode. Taking into account that it is necessary to control solely four IGBTs during each mode (buck or boost), four independent carriers are necessary. In addition, as the MMB dc-dc converter operates with an interleaved feature, the four carriers must present a phase-shift of 90 degrees between each other. Fig. 3 shows the four carriers (tri_A, tri_B, tri_C, and tri_D) and the reference signal (v_{PWM}, which corresponds to the reference voltage v_{xy} established in the control equations). As result of the comparison, Fig. 3 also shows the PWM signals applied, respectively, to the IGBTs s_A, s_B, s_C, and s_D. Obviously, the phase-shift between the four carriers is the same as that between the four PWM signals (s_A, s_B, s_C, and s_D). As it can be seen, due to being considered a duty-cycle value of 75%, there are some periods of time that the PWM signals are overlapping, i.e., times when the IGBTs are turned-on at the same time, since they are turned-on over a time interval of $3T_{sw}/4$.

On the other hand, as can be seen in Fig. 4, when the duty-cycle is 50% during the operation in buck-mode, there is a threshold situation in which the IGBTs are turned-on during the same time interval ($T_{sw}/2$) maintaining a phase-shift of 90 degrees between carriers. With the objective of verifying the

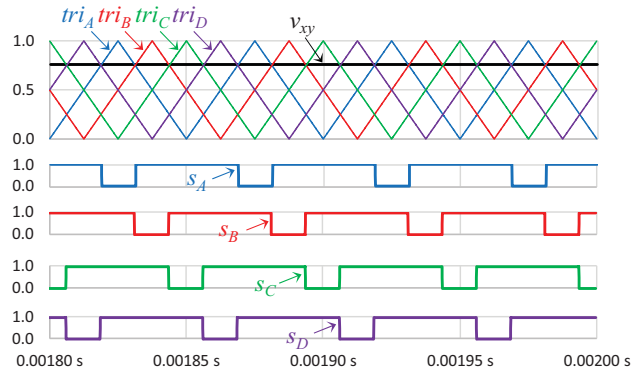

Fig. 3. Pulse-width modulation (PWM) of the MMB dc-dc converter considering a duty-cycle of 75% and operating in buck-mode: Triangular carriers (tri_A, tri_B, tri_C, tri_D); Gate-pulse patterns of the IGBTs (s_A, s_B, s_C, s_D) during the buck-mode operation.

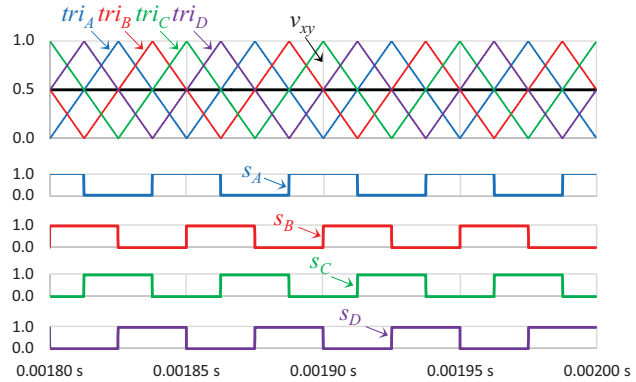

Fig. 4. Pulse-width modulation (PWM) of the MMB dc-dc converter considering a duty-cycle of 50% and operating in buck-mode: Triangular carriers (tri_A, tri_B, tri_C, tri_D); Gate-pulse patterns of the IGBTs (s_A, s_B, s_C, s_D) during the buck-mode operation.

behavior of the PWM with duty-cycle inferior to 50%, Fig. 5 shows the results when the duty-cycle is 25% during operation in boost-mode. In contrast with the situation reported in Fig. 3, when the duty-cycle is 25%, the exact opposite situation occurs, i.e., the PWM signals are never overlapping (IGBTs are never turned-on at the same time, since they are turned-on during a time interval of $T_{sw}/4$), despite the phase-shift of 90 degrees in the carriers.

A. Buck-Mode: Steady-State Operation

Fig. 6 shows the operation of the MMB dc-dc converter during the steady-state operation with a power of 4.5 kW, where a voltage value of 800 V was considered on the interface dc#1 (400 V in $v_{dc\#1,1}$ and in $v_{dc\#1,2}$) and a voltage value of 450 V on the interface dc#2. The output current has been controlled to a value of 10 A. As it can be seen, the voltage of the converter varies between 400 V and 600 V due to the voltage levels of the dc#1 and dc#2 interfaces. This figure also shows the current in each IGBT, and it turns out that the MMB dc-dc converter operates with a duty-cycle value (D) near 50% (due to the voltage value at each dc interface). In more detail, this figure also shows the current at the output $i_{L\{1,2\}}$ and the current in the IGBTs. As shown, the output current $i_{L\{1,2\}}$ has a ripple whose frequency corresponds to four times the switching

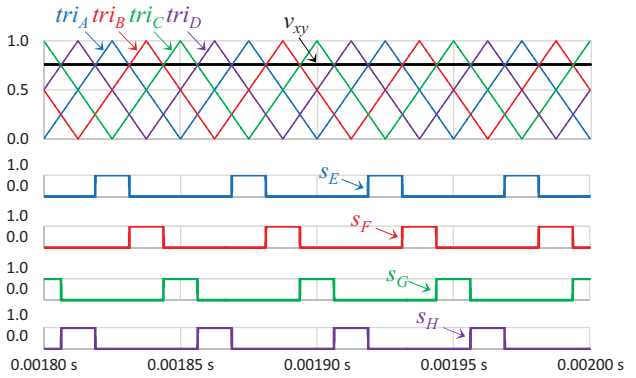

Fig. 5. Pulse-width modulation (PWM) of the MMB dc-dc converter considering a duty-cycle of 25% and operating in boost-mode: Triangular carriers (tri_A, tri_B, tri_C, tri_D); Gate-pulse patterns of the IGBTs (s_A, s_B, s_C, s_D) during the buck-mode operation.

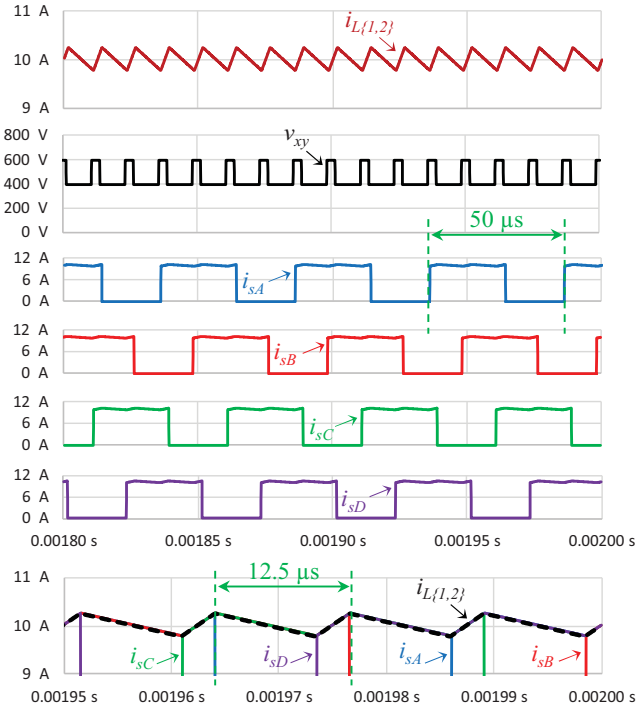

Fig. 6. Steady-state operation of the MMB dc-dc converter during buck-mode: Current in the inductor ($i_{L\{1,2\}}$); Produced voltage (v_{xy}); Current in each IGBT (i_{sA}, i_{sB}, i_{sC}, i_{sD}).

frequency of each IGBT, illustrating the principle of operation in interleaved mode.

Fig. 7 shows a particular situation in which a voltage of 400 V was considered in the interface dc#2, meaning that the MMB dc-dc converter operates with a duty-cycle value of 50%. Therefore, as expected, the output current $i_{L\{1,2\}}$ has a zero current ripple. In this figure, it is also possible to verify the voltage applied to each IGBT, and it is verified that this voltage corresponds to 200 V (voltage in each half of the split dc-link in the interfaces dc#1,1 and dc#1,2).

B. Buck-Mode: Transient-State Operation

Fig. 8 shows the main results during the transient-state operation in buck-mode with a power range between 4.5 kW and 2.25 kW. In this situation, a voltage value of 800 V was

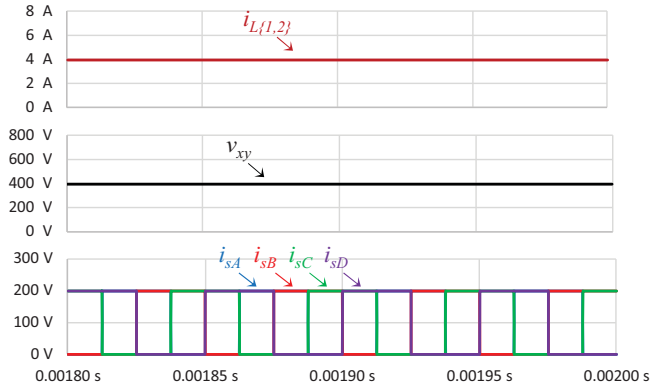

Fig. 7. Steady-state operation of the MMB dc-dc converter during buck-mode: Current in the inductor ($i_{L\{1,2\}}$); Produced voltage (v_{xy}); Voltage in each IGBT (v_{sA}, v_{sB}, v_{sC}, v_{sD}).

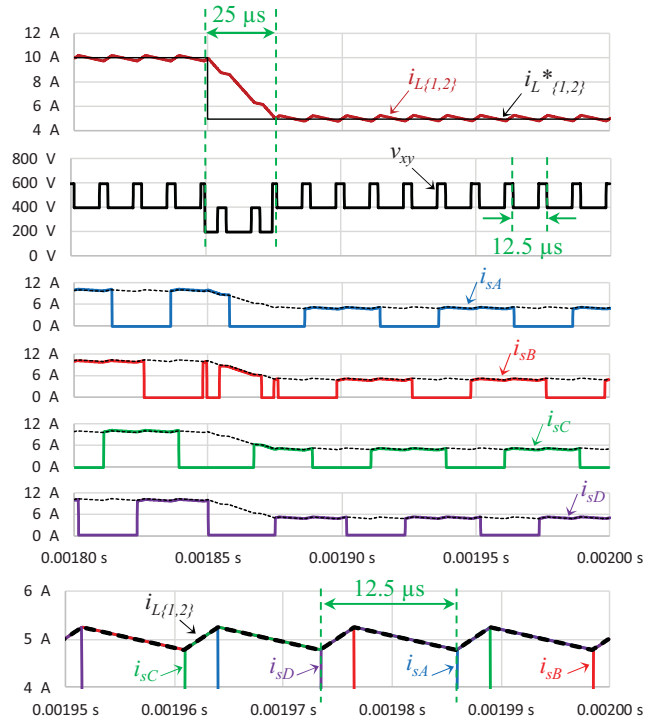

Fig. 8. Transient-state operation of the MMB dc-dc converter during buck-mode: Current in the inductor ($i_{L\{1,2\}}$); Produced voltage (v_{xy}); Current in each IGBT (i_{sA}, i_{sB}, i_{sC}, i_{sD}).

considered at the interface dc#1 and a voltage value of 450 V at the interface dc#2. However, initially a reference current with a value of 10 A was considered and, at 1.85 ms, the reference value was reduced by 50% (i.e., to a value of 5 A). Initially, the current follows the reference and, when the sudden transition occurs, the current takes 25 µs until it reaches again the steady-state (i.e., it takes about one control period). As shown and expected, the current in each IGBT follows the sudden transition. It is of particular interest to visualize that the voltage produced by the converter varies between different levels due to the sudden transition, where the values of 200 V, 400 V and 600 V are assumed. This situation is related to the fact that the converter has to react quickly aiming to changing its current according to the reference. A detail of the current at the output $i_{L\{1,2\}}$, as well as the current in each IGBT, is also shown in this

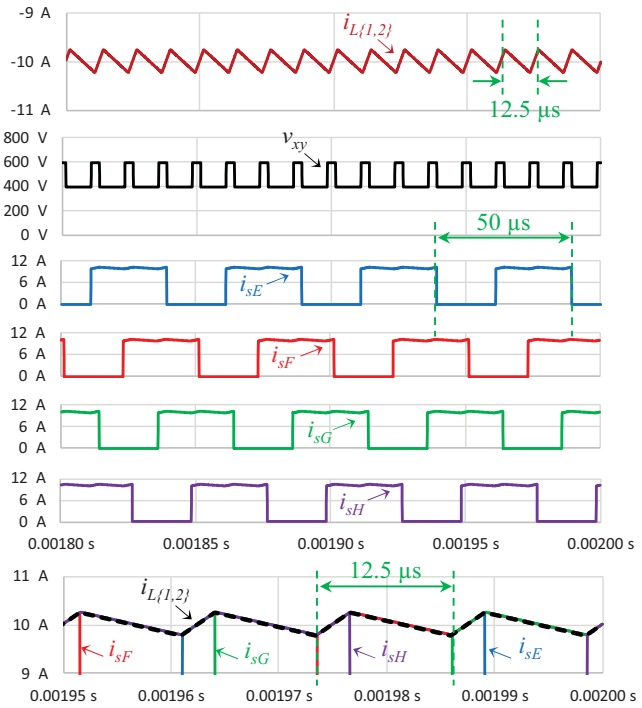

Fig. 9. Steady-state operation of the MMB dc-dc converter during boost-mode: Current in the inductor ($i_{L\{1,2\}}$); Produced voltage (v_{xy}); Current in each IGBT (i_{sE}, i_{sF}, i_{sG}, i_{sH}).

figure, showing that the MMB dc-dc converter maintains the interleaved features even with the sudden transition in the reference current.

C. Boost-Mode: Steady-State Operation

Fig. 9 shows the operation of the MMB dc-dc converter during the steady-state operation in boost-mode with a power of 3.5 kW, where a voltage value of 800 V was considered on the interface dc#1 (400 V in $v_{dc\#1,1}$ and in $v_{dc\#1,2}$) and a voltage value of 350 V on the interface dc#2. As shown, the output current has been controlled to a value of 10 A (it is important to note that the negative value of the current is only due to the position of the current sensor), while the voltage of the converter varies between 400 V and 600 V. This figure also shows the current in each IGBT, as well as a detail of the current at the input $i_{L\{1,2\}}$ and the current in the IGBTs. Also in this mode, the current $i_{L\{1,2\}}$ has a ripple whose frequency corresponds to four times the switching frequency of each IGBT, illustrating the principle of operation in interleaved mode also in boost-mode.

D. Boost-Mode: Transient-State Operation

Fig. 10 shows the main results during the transient-state operation in boost-mode with a power range between 3.5 kW and 875 W. The voltage conditions during the steady-state were also considered in this situation, however, it was considered a sudden transition in the reference current from 10 A to 2.5 A. As shown, also in boost-mode, the current takes 25 µs until it reaches again the steady-state and the current in each IGBT follows the sudden transition. It is of particular interest to visualize that the voltage produced by the converter varies between different levels, due to the sudden transition. By quite

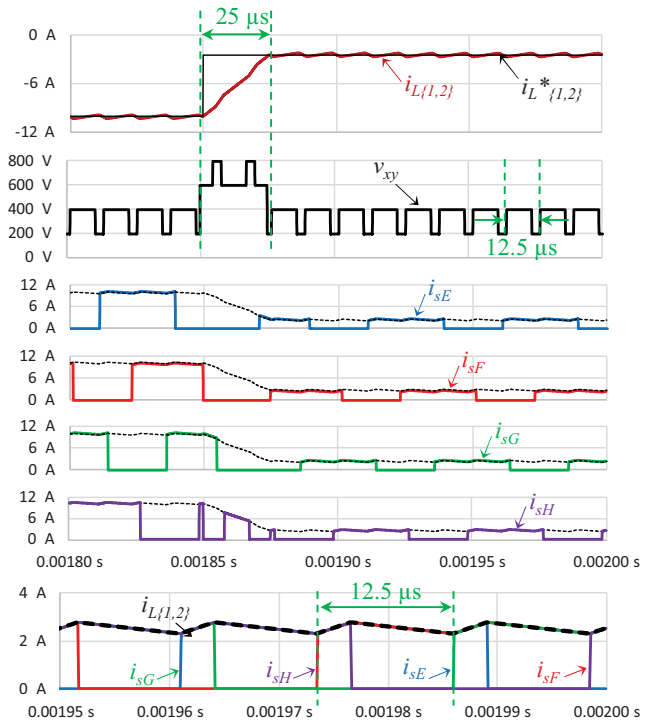

Fig. 10. Transient-state operation of the MMB dc-dc converter during boost-mode: Current in the inductor ($i_{L\{1,2\}}$); Produced voltage (v_{xy}); Current in each IGBT (i_{sE}, i_{sF}, i_{sG}, i_{sH}).

the opposite in relation to the sudden transition in the buck-mode, in this case the produced voltage assumes the values of 200 V, 400 V, 600 V and 800 V. This is caused by the sudden transition, where the reference current was reduced 75%. A detail of the current $i_{L\{1,2\}}$, as well as the current in each IGBT, is also shown in this figure, showing that the MMB dc-dc converter maintains the interleaved features even with the sudden transition in the reference current.

V. Conclusions

A novel topology of a modular multilevel bidirectional (MMB) non-isolated dc-dc converter is proposed for several power electronics applications in smart grids, including renewables, electric mobility, energy storage systems and hybrid power grids. The analysis of the principle of operation is established and the proposed voltage and current control strategies are presented, as well as the pulse-width modulation. As demonstrated along the paper, the proposed MMB dc-dc converter has as main advantageous characteristics the possibility of operating with multilevel voltage and as an interleaved structure. The validation of the MMB dc-dc converter was achieved during the operation in buck-mode and boost-mode for a maximum operating power of 4.5 kW and a switching frequency of 20 kHz, and controlling the current. Furthermore, it was also considered the operation in steady-state and transient-state, showing the dynamic behavior of the voltage levels synthesized by the MMB dc-dc converter, while preserving the interleaved feature. The obtained results in the distinct conditions of operation validate the claimed advantages of the proposed MMB dc-dc converter.

Acknowledgment

This work has been supported by FCT – Fundação para a Ciência e Tecnologia within the R&D Units Project Scope: UIDB/00319/2020. This work has been supported by the FCT Project newERA4GRIDs PTDC/EEI-EEE/30283/2017, and by the FCT Project DAIPESEV PTDC/EEI-EEE/30382/2017. Tiago Sousa is supported by the doctoral scholarship SFRH/BD/134353/2017 granted by FCT.

References

[1] Vehbi C. Gungor, Dilan Sahin, Taskin Kocak, Salih Ergut, Concettina Buccella, Carlo Cecati, Gerhard P. Hancke, “Smart Grid and Smart Homes - Key Players and Pilot Projects,” IEEE Ind. Electron. Mag., vol.6, pp.18-34, Dec. 2012.

[2] Frede Blaabjerg, Josep M. Guerrero, “Smart Grid and Renewable Energy Systems,” ICEMS International Conference on Electrical Machines and Systems, pp.1-10, Aug. 2011.

[3] A. P. Sakis Meliopoulos, George Cokkinides, Renke Huang, Evangelos Farantatos, Sungyun Choi, Yonghee Lee, Xuebei Yu, “Smart Grid Technologies for Autonomous Operation and Control,” IEEE Trans. Smart Grid, vol.2, no.1, pp.1-10, Mar. 2011.

[4] Marcelo Masera, Ettore F. Bompard, Francesco Profumo, Nouredine Hadjsaid, “Smart (Electricity) Grids for Smart Cities: Assessing Roles and Societal Impacts,” Proc. IEEE, vol.106, no.4, pp.613-625, Apr. 2018.

[5] Jing Zhang, “Power Electronics in Future Electrical Power Grid,” IEEE PEDG International Symposium on Power Electronics for Distributed Generation Systems, pp.1-3, July 2013.

[6] Ma Zhengyou, “Study on the Application of Advanced Power Electronics in Smart Grid,” IEEE FGCT International Conference on Future Generation Communication Technologies, pp.96-99, 2017.

[7] An Luo, Qianming Xu, Fujun Ma, Yandong Chen, “Overview of Power Quality Analysis and Control Technology for the Smart Grid,” SPRINGER Journal of Modern Power Systems and Clean Energy, vol.4, no.1, pp.1-9, Jan. 2016.

[8] Jonas E. Huber, Johann W. Kolar, “Applicability of Solid-State Transformers in Today’s and Future Distribution Grids,” IEEE Trans. Smart Grid, vol.10, no.1, pp.317-326, Jan. 2019.

[9] Vitor Monteiro, J. G. Pinto, Joao L. Afonso, “Experimental Validation of a Three-Port Integrated Topology to Interface Electric Vehicles and Renewables with the Electrical Grid”, IEEE Trans. Ind. Informat., vol.14, no.6, pp 2364-2374, June 2018.

[10] Farzam Nejabatkhah, Yun Wei Li, And Hao Tian, “Power Quality Control of Smart Hybrid AC/DC Microgrids: An Overview,” IEEE Access, vol.7, pp.52295-52318, Apr. 2019.

[11] Navid Bayati , Amin Hajizadeh, Mohsen Soltani, “Protection in DC microgrids: a comparative review,” IET Smart Grid, vol.1, no.3, pp.66-75, Sept. 2018.

[12] Vitor Monteiro, Joao C. Ferreira, Andres A. Nogueiras Melendez, Carlos Couto, Joao L. Afonso, “Experimental Validation of a Novel Architecture Based on a Dual-Stage Converter for Off-Board Fast Battery Chargers of Electric Vehicles,” IEEE Trans. Veh. Tech., vol.67, no.2, pp.1000-1011, Feb. 2018.

[13] Vitor Monteiro, Bruno Exposto, Joao C. Ferreira, Joao L. Afonso, “Improved Vehicle-to-Home (iV2H) Operation Mode: Experimental Analysis of the Electric Vehicle as Off-Line UPS,” IEEE Transactions on Smart Grid, vol.8, no.6, pp.2702-2711, Nov. 2017.

[14] Vitor Monteiro, Joao C. Ferreira, Andres A. Nogueiras Melendez, Joao L. Afonso, “Model Predictive Control Applied to an Improved Five-Level Bidirectional Converter,” IEEE Trans. Ind. Electron., vol.63, no.9, pp.5879-5890, Sept. 2016.

[15] Saman A. Gorji, Hosein G. Sahebi, Mehran Ektesabi, And Ahmad, B. Rad, “Topologies and Control Schemes of Bidirectional DC–DC Power Converters: An Overview,” IEEE ACCESS, vol.7, pp117997-118019, Aug. 2019.

[16] Juan David Paez, David Frey, Jose Maneiro, Seddik Bacha, Piotr Dworakowski, “Overview of DC–DC Converters Dedicated to HVdc Grids,” IEEE Trans. Power Del., vo.34, no.1, pp.119-128, Feb. 2019.

[17] Monika Singhal, Naresh K Pilli, S. K. Singh, “Modeling and Analysis of Split-Pi Converter Using State Space Averaging Technique,” IEEE PEDES International Conference on Power Electronics, Drives and Energy Systems, pp.1-6, 2014.

[18] D. Sabatta, J. Meyer, “Super Capacitor Management Using a Split-Pi Symmetrical Bi- directional DC-DC Power Converter with Feed-Forward Gain Control,” IEEE International Conference on the Domestic Use of Energy, Abr. 2018.

[19] Tanvir Ahmad, Sharmin Sobhan,“Performance Analysis of Bidirectional Split-Pi Converter Integrated with Passive Ripple Cancelling Circuit,” IEEE ECCE Conference on Electrical, Computer and Communication Engineering (ECCE), pp.433-437, Bangladesh, Feb. 2017.

[20] Sharmin Sobhan, Khandaker Lubaba Bashar, “A Novel Split-Pi Converter with High Step-up Ratio Sharmin,” IEEE Region 10 Humanitarian Technology Conference, pp.255-258, 21-23 Dec. 2017.

[21] Ahmad Alzahrani, Pourya Shamsi, Mehdi Ferdowsi, “Single and Interleaved Split-pi DC-DC Converter,” IEEE International Conference on Renewable Energy Research and Applications, pp.995-1000, CA USA, Nov. 2017.